Rapid thermo-optical quality assessment of laser gain media

Christina C C Willis,[1,2] Joshua D Bradford,[1] John Haussermann,[3] Erik McKee,[1,4] Emily Maddox,[1] Lawrence Shah,[1] Romain Gaume,[1] and Martin Richardson[1,*]

[1]*College of Optics, CREOL, University of Central Florida, 304 Scorpius Street, Orlando, FL 32816, USA*
[2]*Currently with Fibertek, 13605 Dulles Technology Dr., Herndon, VA 20171, USA*
[3]*Department of Mathematics, University of Central Florida, 4393 Andromeda Loop N., Orlando, FL 32816, USA*
[4]*Currently with TRUMPF Inc., Farmington Industrial Park, Farmington, CT 06032, USA*
[*]*mcr@creol.ucf.edu*

Abstract: We describe a technique for the quick and simple assessment of doped optical materials for use as laser gain media. To demonstrate this technique, referred to as Rapid Thermo-Optical Assessment (RTOA), we analyze a set of ceramic and crystalline Yb^{3+}:YAG samples. RTOA is based on Shack-Hartmann wavefront sensing and thermal lensing to evaluate the media's thermal response, giving a relative overall quality assessment of the material. The technique is also broadly applicable to optical media considered for high power or thermal loading conditions, and useful for the refinement of fabrication methods.

OCIS codes: (140.6810) Thermal effects; (140.3380) Laser materials; (350.6830) Thermal lensing; (350.5340) Photothermal effects.

References and links

1. A. W. AlShaer, L. Li, and A. Mistry, "The effects of short pulse laser surface cleaning on porosity formation and reduction in laser welding of aluminum alloy for automotive component manufacture," Opt. Laser Technol. **64**, 162–171 (2014).
2. G. Boulon, "Fifty years of advances in solid-state laser materials," Opt. Mater. **34**(3), 499–512 (2012).
3. Office of Naval Research, "All Systems Go: Navy's Laser Weapon Ready for Summer Deployment," http://www.navy.mil/submit/display.asp?story_id=80172.
4. J. Sanghera, S. Bayya, G. Villalobos, W. Kim, J. Frantz, B. Shaw, B. Sadowski, R. Miklos, C. Baker, M. Hunt, I. Aggarwal, F. Kung, D. Reicher, S. Peplinski, A. Ogloza, P. Langston, C. Lamar, P. Varmette, M. Dubinskiy, and L. DeSandre, "Transparent ceramics for high-energy laser systems," Opt. Mater. **33**(3), 511–518 (2011).
5. A. Ikesue, T. Kinoshita, K. Kamata, and K. Yoshida, "Fabrication and Optical Properties of High-Performance Polycrystalline Nd:YAG Ceramics for Solid-State Lasers," J. Am. Ceram. Soc. **78**(4), 1033–1040 (1995).
6. A. Alexandrovski, M. Fejer, A. Markosian, and R. Route, "Photothermal common-path interferometry (PCI): new developments," in *Solid State Lasers XVIII: Technology and Devices,* W. A. Clarkson, N. Hodgson, and R. K. Shori, eds. (SPIE, 2009), pp. 71930D.
7. R. Gaume, Y. He, A. Markosyan, and R. L. Byer, "Effect of Si-induced defects on 1 μm absorption losses in laser-grade YAG ceramics," J. Appl. Phys. **111**(9), 093104 (2012).
8. F. Zhuang, B. Jungbluth, B. Gronloh, H. D. Hoffmann, and G. Zhang, "Dual-wavelength, continuous-wave Yb:YAG laser for high-resolution photothermal common-path interferometry," Appl. Opt. **52**(21), 5171–5177 (2013).
9. N. J. Dovichi and J. M. Harris, "Laser induced thermal lens effect for calorimetric trace analysis," Anal. Chem. **51**(6), 728–731 (1979).
10. S. Chenais, F. Balembois, F. Druon, G. Lucas-Leclin, and P. Georges, "Thermal lensing in diode-pumped ytterbium Lasers-Part I: theoretical analysis and wavefront measurements," IEEE J. Quantum Electron. **40**(9), 1217–1234 (2004).
11. S. Chenais, F. Balembois, F. Druon, G. Lucas-Leclin, and P. Georges, "Thermal lensing in diode-pumped ytterbium Lasers-Part II: evaluation of quantum efficiencies and thermo-optic coefficients," IEEE J. Quantum Electron. **40**(9), 1235–1243 (2004).
12. C. Jacinto, A. A. Andrade, T. Catunda, S. M. Lima, and M. L. Baesso, "Thermal lens spectroscopy of Nd:YAG," Appl. Phys. Lett. **86**(3), 034104 (2005).
13. C. Jacinto, T. Catunda, D. Jaque, L. E. Bausá, and J. García-Solé, "Thermal lens and heat generation of Nd:YAG lasers operating at 1.064 and 1.34 μm," Opt. Express **16**(9), 6317–6323 (2008).
14. F. Druon, S. Ricaud, D. N. Papadopoulos, A. Pellegrina, P. Camy, J. L. Doualan, R. Moncorge, A. Courjaud, E. Mottay, and P. Georges, "On Yb:CaF2 and Yb:SrF_2: review of spectroscopic and thermal properties and their impact on femtosecond and high power laser performance," Opt. Mater. Express **1**(3), 489–502 (2011).

#235182 - $15.00 USD Received 2 Mar 2015; revised 7 May 2015; accepted 8 May 2015; published 19 May 2015

15. W. F. Krupke, M. D. Shinn, J. E. Marion, J. A. Caird, and S. E. Stokowski, "Spectroscopic, optical, and thermomechanical properties of neodymium- and chromium-doped gadolinium scandium gallium garnet," J. Opt. Soc. Am. B **3**(1), 102–114 (1986).
16. F. D. Patel, E. C. Honea, J. Speth, S. A. Payne, R. Hutcheson, and R. Equall, "Laser demonstration of $Yb_3Al_5O_{12}$ (YbAG) and materials properties of highly doped Yb:YAG," IEEE J. Quantum Electron. **37**(1), 135–144 (2001).
17. D. P. Devor, L. G. DeShazer, and R. C. Pastor, "Nd:YAG quantum efficiency and related radiative properties," IEEE J. Quantum Electron. **25**(8), 1863–1873 (1989).
18. M. Ito, C. Goutaudier, Y. Guyot, K. Lebbou, T. Fukuda, and G. Boulon, "Crystal growth, Yb^{3+} spectroscopy, concentration quenching analysis and potentiality of laser emission in $Ca_{1-X}Yb_XF_{2+X}$," J. Phys: Condens. Mat. **16**, 1501 (2004).
19. C. C. C. Willis, J. Bradford, L. Shah, and M. Richardson, "Measurement of Wavefront Distortions Resulting from Incidence of High-Power 2 μm Laser Light," in *Solid State and Diode Laser Technology Review* (Directed Energy Professional Society, 2011).
20. C. C. C. Willis, J. D. Bradford, E. Maddox, L. Shah, and M. Richardson, "Thermo-optic quality assessment of doped optical ceramics," in *Solid State Lasers XXII: Technology and Devices* (SPIE, 2013), pp. 85990.
21. A. Ikesue and Y. L. Aung, "Ceramic Laser Materials," Nat. Photonics **2**(12), 721–727 (2008).
22. K. A. Appiagyei, G. L. Messing, and J. Q. Dumm, "Aqueous slip casting of transparent yttrium aluminum garnet (YAG) ceramics," Ceram. Int. **34**(5), 1309–1313 (2008).
23. A. Ikesue, Y. L. Aung, T. Yoda, S. Nakayama, and T. Kamimura, "Fabrication and laser performance of polycrystal and single crystal Nd:YAG by advanced ceramic processing," Opt. Mater. **29**(10), 1289–1294 (2007).
24. J. Zhang, L. An, M. Liu, S. Shimai, and S. Wang, "Sintering of Yb^{3+}:Y_2O_3 transparent ceramics in hydrogen atmosphere," J. Eur. Ceram. Soc. **29**(2), 305–309 (2009).
25. J. Lu, K. Takaichi, T. Umematsu, A. Skirawa, M. Musha, K. Ueda, H. Yagi, T. Yanagitami, and A. A. Kaminskii, "Yb^{3+}:Y_2O_3 Ceramics–A Novel Solid-State Laser Material," Jpn. J. Appl. Phys. **41**(2), 1373–1375 (2002).
26. W. Zhang, T. Lu, N. Wei, B. Ma, F. Li, Z. Lu, and J. Qi, "Effect of annealing on the optical properties of Nd: YAG transparent ceramics," Opt. Mater. **34**(4), 685–690 (2012).
27. S. R. Rotman, C. Warde, H. L. Tuller, and J. Haggerty, "Defect-property correlations in garnet crystals. V. Energy transfer in luminescent yttrium aluminum–yttrium iron garnet solid solutions," J. Appl. Phys. **66**(7), 3207–3210 (1989).
28. A. K. Cousins, "Temperature and thermal stress scaling in finite-length end-pumped laser rods," IEEE J. Quantum Electron. **28**(4), 1057–1069 (1992).
29. W. Koechner, *Solid-State Laser Engineering* (Springer, 2006).
30. W. F. Krupke, "Ytterbium solid-state lasers. The first decade," IEEE J. Sel. Top. Quant. **6**(6), 1287–1296 (2000).
31. S. Chenais, F. Druon, S. Forget, F. Balembois, and P. Georges, "On thermal effects in solid-state lasers: The case of ytterbium-doped materials," Prog. Quantum Electron. **30**(4), 89–153 (2006).
32. G. Ranganath and S. Ramaseshan, "Photoelasticity in polycrystalline aggregates," Pramana **1**(2), 78–87 (1973).

1. Introduction

High-power pulsed and CW lasers are used in many industrial, scientific, and military applications [1–3]. The high fluences encountered in these systems lead to thermal distortions in intra- and extra-cavity optics, which can degrade laser performance, potentially causing catastrophic damage [4]. It is critical to ensure that the optical media employed in high power laser systems exhibit the minimum possible distortion under high optical loads, and therefore necessary to have analysis techniques for evaluating and selecting such materials.

Various methods already exist for assessing optical material quality, with high quality being defined here as an absence of impurities that contribute to additional thermal loading. To determine the suitability of material as laser gain media, a common method of assessment is to characterize a sample's performance directly in a laser cavity. This method is straightforward; however, it requires complete fabrication and optical coating of the sample, as well as assembly and alignment of the laser cavity [5]. So while it offers a complete picture of sample suitability, it is relatively costly and time consuming. Other methods of analysis that offer quantitative evaluation of specific material properties include: photothermal commonpath interferometry (PCI) [6–8], various thermal lensing techniques [9–11] including mode-mismatched thermal lens spectrometry [12, 13], emission and absorption spectral measurements [14, 15], x-ray diffraction [4], calorimetry [16], interferometric measurement [17], and fluorescence lifetime measurement [14, 18]. And while these techniques can offer absolute measurements of certain materials parameters, none of them offer an integrated picture of the overall material quality.

#235182 - $15.00 USD Received 2 Mar 2015; revised 7 May 2015; accepted 8 May 2015; published 19 May 2015

The thermo-optical characterization technique described herein, referred to as Rapid Thermo-Optical Assessment (RTOA), is a repeatable and highly sensitive measurement technique that can be used to quickly establish an integrated picture of a sample's overall quality in terms of thermal distortion. This technique does not require any a priori knowledge of specific material thermo-mechanical properties or the use of a quantified reference sample. Its simple experimental setup consists of a powerful CW pump beam to heat the samples, and a low power probe beam for Shack-Hartmann Wavefront Sensing (SHWFS) measurements. The measured thermal lensing can be used to rank a samples relative to others of its type, and be cross-referenced as needed against an ideal model i.e. one that assumes no impurities. The extent to which the sample's thermal response deviates from its model can be taken as a direct indication of its overall thermo-optical quality, and/or a process of elimination can be performed based on the ranking of a sample set.

RTOA is unique in that it offers an overall sample quality measurement while employing a simple experimental set up. Both PCI and RTOA can be used to evaluate a wide variety of material types, but RTOA offers integrated quality measurement without a complicated interferometric set up. The powerful thermal lensing technique outlined by Chenais et al. [10, 11], in contrast to RTOA, can be used to measure a variety of material properties in absolute terms. However, it also has a more complex experimental setup than RTOA, including a laser cavity, and its overall accuracy is dependent upon its cavity mode and probe beam being the same size in the test sample. The experimental set up and analysis method defined as RTOA was developed from a series of prior works [19, 20] which evolved into the robust and repeatable methodology presented herein.

To the best of the authors' knowledge no technique comparable to RTOA currently exists, either with respect to its particular experimental and analytical methodology, or in terms of its simple measurement of thermal response for high optical-loading applications. It is versatile in that either a single sample can be compared to its ideal model, or a set of samples can be ranked in terms of quality with high precision. RTOA is not only useful for the end user of optical materials, who designs and builds optical systems, but also, and especially, for the materials scientist who fabricates optical ceramics, allowing for swift troubleshooting and improvement of fabrication methods and materials.

As a demonstration of the capabilities of RTOA, thermally-induced distortions were measured in a set of 13 laser-grade ceramic and single-crystal Yb:YAG samples. Optical-quality ceramic laser materials are an excellent subject for RTOA because of their many uses in high power applications [21], and because they are sensitive to different fabrication methods and starting materials [22–25]. For example, when the starting materials for the fabrication of ceramics are 99.99% pure, impurities of 0.05-0.08 wt. ppm have been observed [18], which is enough to degrade thermo-optic properties. Here we demonstrate that the RTOA technique has sufficient sensitivity to be able to detect both large and small variations between samples, and to determine the overall sample quality.

2. Yb:YAG samples and RTOA experimental setup

A total of 13 ceramic and crystalline Yb:YAG samples were examined for this study. All samples are thin circular Yb^{3+}:YAG disks (Table 1) with similar surface polish (scratch-dig: 20-10, parallelism: ≤ 5 arcsec, surface quality: λ/10). The samples originated from 4 different sources, including both single crystal and polycrystalline material, thus representing different starting materials and processing techniques. There is some variation in sample diameter and thickness, and to a small extent dopant concentration; the effects of these differences are addressed in subsequent sections.

During testing, each sample was held in a water-cooled aluminum mount, Fig. 1, maintained at 13°C. The water cooling was important as it allowed the samples to reach a thermal equilibrium by maintaining the sample edge at a constant temperature. The mount consisted of two aluminum plates with equivalent clear apertures that clamp the target samples at their periphery, with a pair of plates matched to each sample diameter. This

#235182 - $15.00 USD Received 2 Mar 2015; revised 7 May 2015; accepted 8 May 2015; published 19 May 2015

arrangement also provided mechanical stability and repeatability by ensuring that each sample was centered on the same location.

A 940 nm high-power fiber-coupled diode was used to heat the samples at a 30° angle of incidence, and was focused to a ~2 mm diameter spot in the center of the sample. To ensure centration of the pump in each sample, once the pump beam was aligned to the center of the mount, no changes were made to mount position or beam alignment, which allows measurements to be performed quickly with good experimental uniformity. The pump spot size was selected to be smaller than the clear aperture of the samples in order to reduce the impact of the radial variation on the measurements, as well as to reduce any potential variation in boundary conditions created by the clamping of the mount. While it is useful to have the pump spot be small to reduce these effects, the absolute pump spot size is less important than its consistency of size across all samples.

Table 1. List of samples tested

Label	Source	Material	Dopant conc. (at%)	Diameter (mm)	Thickness (mm)
Sample 1	1	ceramic	9.8	18.0	1.24
Sample 2	1	ceramic	9.8	18.0	1.23
Sample 3	1	ceramic	9.8	18.0	1.23
Sample 4	1	ceramic	9.8	18.0	1.23
Sample 5	1	crystal	9.8	17.9	1.31
Sample 6	1	crystal	9.8	18.0	1.35
Sample 7	2	ceramic	10	18.4	1.40
Sample 8	2	ceramic	10	18.3	1.39
Sample 9	2	ceramic	10	18.5	1.39
Sample 10	3	ceramic	9.8	21.1	1.39
Sample 11	3	Ceramic	9.8	31.1	1.53
Sample 12	3	Crystal	9.8	20.0	1.59
Sample 13	4	Ceramic	10	41.1	2.16

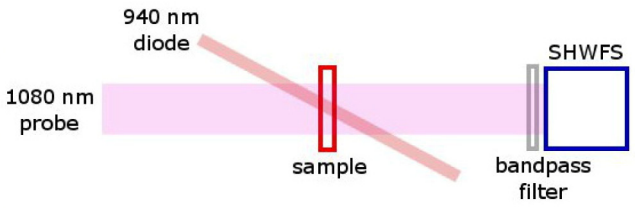

(a) (b)

Fig. 1. a) Water-cooled sample mount, b) diagram of RTOA measurement setup.

A 30 mW probe beam centered spectrally at 1080 nm was delivered by a fiber-coupled diode. The wavelength of the probe was selected to offset the probe spectrally from the pump and allow for filtering of the pump light with a bandpass filter, preventing pump light from affecting the measurements. Yb:YAG also has a low absorption coefficient at 1080 nm, which, combined with the low power of the probe, ensures that it has a negligible contribution to the thermal load. The probe was collimated to a ~15 mm diameter spot size and transmitted through the sample onto the SHWFS (Imagine Optic HASO First). This size matched the clear aperture of the smallest samples and was kept at this size for all samples for maximum consistency. The induced wavefront distortion was measured in steps of applied pump power, from 1 to 30 W incident on the sample.

#235182 - $15.00 USD Received 2 Mar 2015; revised 7 May 2015; accepted 8 May 2015; published 19 May 2015

3. Thermal lensing measurements

Wavefront distortion measurements were taken when thermal equilibrium was established. The resulting wavefront distortions measured were nearly cylindrical, owing to the circular symmetry of the samples, the heat transfer boundary conditions, and the isotropic and cubic symmetries of the polycrystalline and single-crystalline samples respectively. An example of a typically wavefront distortion is shown in Fig. 2.

The resulting shape of the radial thermal profile is dominantly quadratic in nature, both in and immediately surrounding the pumped region. Outside of the pumped region the temperature drops off logarithmically towards the cooled outer boundary. Consequently, the feature of primary interest in the induced wavefront distortion was the average accumulated quadratic phase perturbation, which is associated with the formation of a thermal lens. The radius of curvature of the measured wavefront was used to calculate the focal length and dioptric power of the thermal lens.

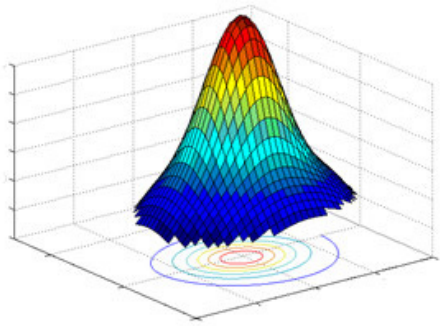

Fig. 2. Example of thermal distortion induced by optical pumping of a sample.

For all samples, the dioptric power of the induced thermal lens increased with an approximately linear relationship to the incident pump power, Fig. 3. Each data point represents the mean of 1 minute of data collection, where each averaged datum is itself the average of 20 acquisitions. This averaging compensates for the noise present in the measurements, caused primarily by ambient airflow. Characteristic error was approximately ± 0.1 to 0.2 diopters for all samples. Values shown are corrected according to sample thickness and the 0.2% variation in dopant concentration. The variation in radial size of the samples cannot be corrected directly here, but is accounted for via the theoretical model discussed in subsequent sections.

A wide range of slopes is observed for the full set of samples. The thermal response of the samples is characterized in terms of their slope, in units of dioptric power per unit of optical pump power, D/W. The differences in the thermal response of the samples (or slope) are interpreted as a variation in the quality of the sample material; and a larger slope value indicates a greater (undesirable) thermal response. All the samples are ostensibly the same material after a correction for their 0.2% variation in dopant concentration. Thus, the variation of their thermal response indicates that there are differences amongst the samples in terms of: 1) absorption at the pump wavelength, 2) the extent to which non-radiative relaxation pathways are present, and 3) the materials' thermal conductivity. These variations are most likely caused by differences in the starting materials or the fabrication methods used by the manufacturers.

In relative terms, it was found that the crystalline materials were the best performers of this particular sample set, with Sample 13 being the lowest performing sample, and Samples 5 and 6 being the best. Due to the dramatic response of Sample 13, testing was stopped short of the full 30 W in order to avoid possible fracture damage to the sample.

#235182 - $15.00 USD Received 2 Mar 2015; revised 7 May 2015; accepted 8 May 2015; published 19 May 2015

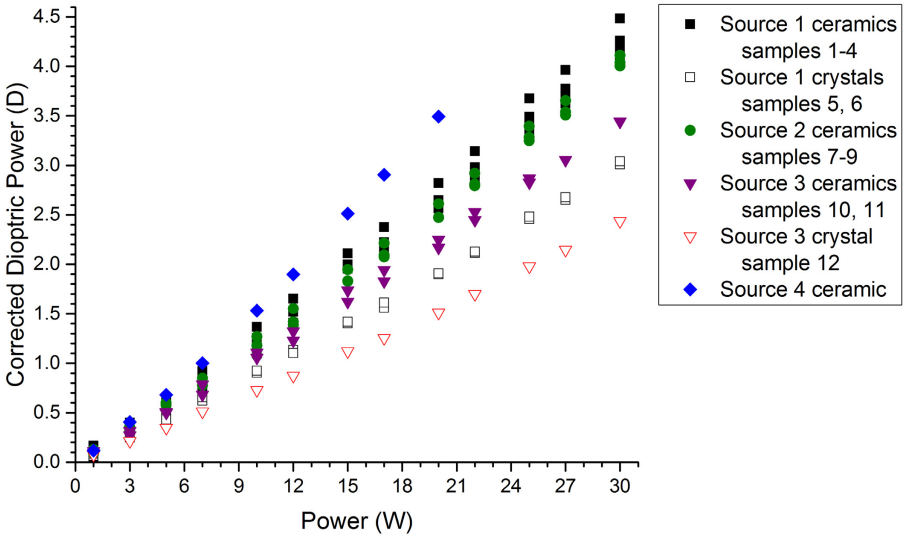

Fig. 3. Dioptric power, corrected for sample length and dopant concentration, of the induced thermal lens as a function of the incident pump power for all samples.

It should also be noted that samples originating from the same source are grouped closely in slope values, indicating a level of self-consistency in the fabrication process for a given manufacturer. If samples from a given source were not closely grouped, the lack of self-consistency would indicate issues with the production quality. As such, one additional application of this technique is to provide a measure of repeatability and reliability of an established fabrication process.

4. Sample transmission spectra

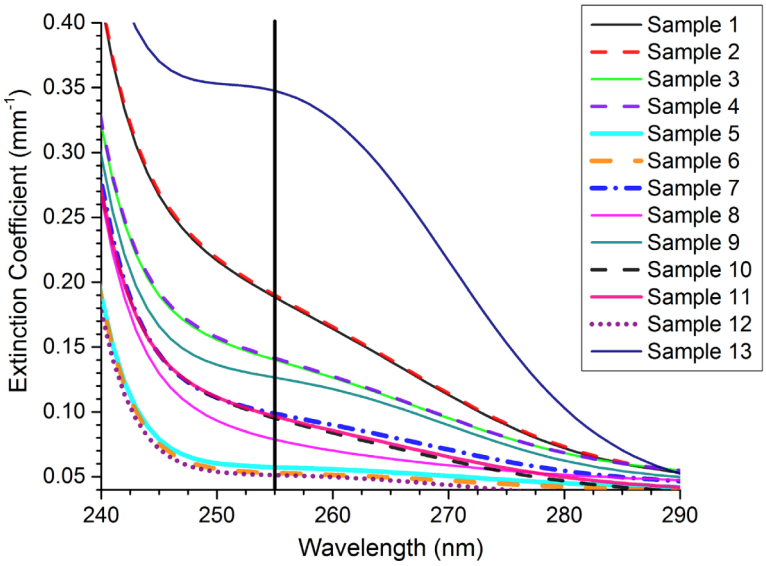

Fig. 4. Extinction feature near 255 nm demonstrates a significant amount of variation between samples.

One possible cause of the observed sample variation is the presence of either chemical impurities or phase impurities in the samples. And such impurities sometimes manifest as

#235182 - $15.00 USD Received 2 Mar 2015; revised 7 May 2015; accepted 8 May 2015; published 19 May 2015

spectral absorption features. To determine if any impurities would be apparent, all samples were measured with a spectrophotometer (Agilent Cary 500) from 200 to 2200 nm. After performing a baseline correction, the extinction coefficient (extinction per unit length) was calculated from the transmission measurements.

All samples had the characteristic Yb^{3+} absorption features from 800 to 1100 nm and there was no significant variation amongst the samples in this spectral range. The only region where notable differences were apparent appeared near 255 nm, which presented itself as a hump in the extinction coefficient, Fig. 4 and is particularly notable in Sample 13. The most likely cause of this feature is Fe^{3+} contamination, which is known to affect material behavior in the UV [26, 27] and is a common component of equipment used for fabricating ceramics. The correlation between this extinction feature and the measured thermal responses of the samples is discussed in the following section.

5. Thermal lensing model and analysis

An analytical model of the thermal lensing was developed in order to address all sample variations, including radial differences, which allowed for a direct comparison between samples. The thermal response of the sample is defined by a linear fit of the sample's distortion as a function of incident power (D/W). While the linear fit is a good approximation for the behavior of all samples ($R^2 \geq 0.995$), Sample 13 exhibits a slightly non-linear response. However, when fitted with a line it has an R^2 of 0.995, and for the purposes of this analysis a linear approximation is used.

In the model, the ideal thermal responses of the samples (assuming no impurities) were analytically generated so that the deviation of the samples from their ideal response could be quantified in terms of Δ(D/W). Here Δ(D/W) represents the difference between a sample's modeled thermal response and its experimentally measured *uncorrected* thermal response, each in units of D/W.

The thermal profile of each sample was generated based on ideal material parameters, sample dimensions, and the experimental conditions (pump intensity, spot size, and cooling). The expressions used for generating the thermal profile are outlined in [28]. A simplifying assumption was made that all heat flow in the sample was radial, with no thermal variation along the direction of propagation. Solely for the purpose of validating this assumption, a COMSOL numerical model that used no simplifications was generated for several samples. Less than 1% variation was found between the two approaches, validating the assumption of radial-only heat flow for our set up.

The unheated region of the sample, which drops logarithmically in temperature from the heated region to the sample edge, does not significantly contribute to the thermal distortion. Consequently, the thermal lens can be represented solely by the parabolic term which describes the thermal profile of the pumped region and its immediate area. This quadratic term was found by performing a parabolic fit to the heated region of the thermal profile, and was substituted into the standard thermal lensing model outlined by Koechner [29] to find the theoretical effective focal length of the induced thermal lens. All materials parameters used in the model were taken from prior literature [10, 29–31], excepting the thermo-optic coefficients for the ceramics, which were calculated using the Hill approximation [32], and a plane stress approximation for the longitudinal pumping of the samples (Table 2). Some variation in materials parameters exists in the literature, but because RTOA is a relative technique, the exact value used for a given property is of less importance than its consistent application.

Table 2. Photoelastic and thermo-optic coefficients for polycrystalline YAG

p11	-0.0627
p12	0.0260
p44	-0.0444
Cr	0.0045
Cθ	-0.0093

#235182 - $15.00 USD Received 2 Mar 2015; revised 7 May 2015; accepted 8 May 2015; published 19 May 2015

The predictions of the model were compared to the results of each sample, four examples of which are shown in Fig. 5; note that the model values are compared to the raw, uncorrected experimental values of the measured thermal lens. The extent to which the experimental data deviates from its modeled ideal, Δ(D/W), is different for each sample. It is beyond the scope of this work to determine a specific cause for the observed deviation, but it likely corresponds to the presence of impurities such as Fe^{3+}, silicon [7] (which is often used as a sintering aid), or oxygen vacancies resulting from insufficient annealing of the ceramics.

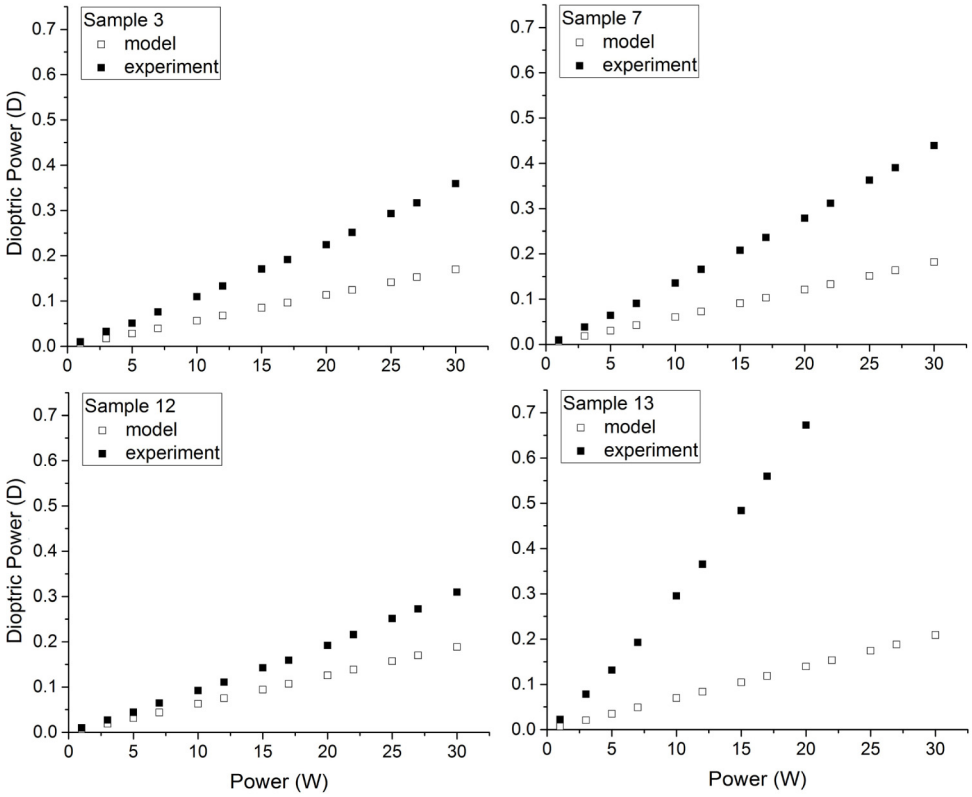

Fig. 5. Representative examples of deviation between experimental sample behavior and thermal model prediction.

When the calculated model deviation values, Δ(D/W), are plotted against *corrected* experimental thermal response values, D/W, a strong positive correlation is observed, Fig. 6. The correlation coefficient of this plot is 0.744, and excluding Sample 13 which is a clear outlier, the coefficient becomes 0.804. It is important to emphasize that this correlation is drawn between experimental values that are corrected for sample thickness and dopant concentration but not radius, as shown in Fig. 3, and the deviation of the raw, uncorrected values from their respective models, as shown in Fig. 5. This strong positive correlation indicates that under these experimental conditions, the radius of the sample plays only a small role in the samples' thermal response. This is because the corrected thermal response values do not account for radial variation and the deviation values do. It also indicates that both methods for quantifying sample response are roughly equivalent, showing both the sensitivity of the measurement and confirming the validity of the model assumptions.

Another interesting correlation is found when the extinction coefficient values at 255 nm are plotted against the samples' thermal response (D/W). A strong positive correlation is observed, in Fig. 7, with a correlation coefficient of 0.865. Three samples (4, 7 and 8) are slightly offset from the general trend, an anomaly we believe is due to increased scattering in

#235182 - $15.00 USD Received 2 Mar 2015; revised 7 May 2015; accepted 8 May 2015; published 19 May 2015

these particular samples. This strong correlation indicates that the impurity associated with the 255 nm extinction feature is a dominant factor in the samples' thermal distortion, but that there exist other factors which are contributing to varying extents.

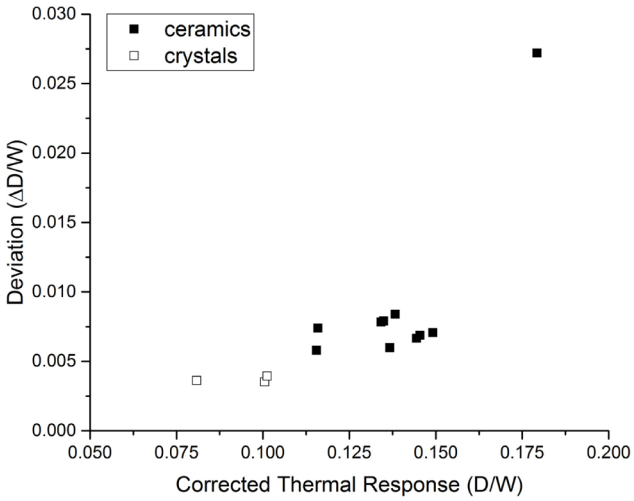

Fig. 6. Model deviation, Δ(D/W), plotted against corrected experimental distortion, D/W, shows a strong positive correlation.

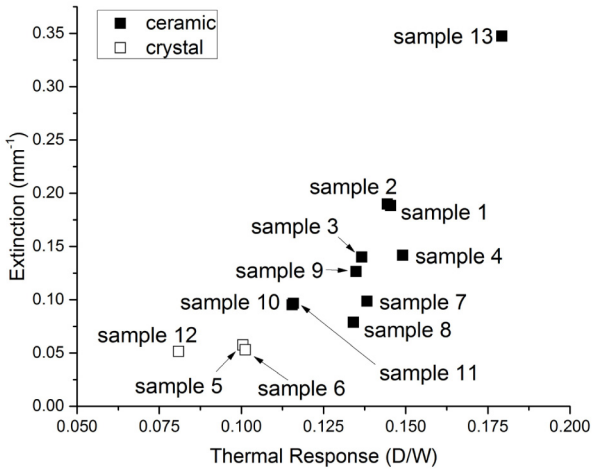

Fig. 7. Relationship between extinction coefficient at 255 nm and sample thermal distortion.

Use of supportive measurements, such as transmission spectra, can be instructive in materials assessment, but are not a substitute for thermal testing with RTOA. While there is a clear correlation between the 255 nm extinction feature and poor thermal performance of the samples, it is not possible to definitively state causality between the two. It is also possible for flaws to exist in a material which may not be visible on a transmission spectrum, which is why transmission spectrum alone cannot be used to determine thermal performance. Further, the correlation with the 255 nm extinction feature in YAG materials may not be applicable to other laser materials. This is what makes RTOA such a powerful technique: it can yield an integrated assessment of material quality by applying a thermal load that is analogous to the sample's prospective operating conditions, as opposed to extrapolating sample behavior from individual measurements of material parameters.

#235182 - $15.00 USD Received 2 Mar 2015; revised 7 May 2015; accepted 8 May 2015; published 19 May 2015

6. Conclusions

We described herein the Rapid Thermo-Optical Analysis (RTOA) technique for assessing sample quality of laser host media using SHWFS, cross-referenced with analytical modeling of the samples' thermal response. The technique was demonstrated by inducing and measuring thermal lensing in a set of 13 Yb^{3+}-doped ceramic and crystalline YAG samples, which allowed for a relative comparison of sample quality. The deviation of the samples from their ideal thermal response was also calculated. A strong positive correlation (0.804) was noted between the corrected experimental thermal response (D/W) and the model deviation Δ(D/W) of the samples, which validated the model and demonstrated the sensitivity of the measurement technique.

The presence of an extinction feature in sample transmission at 255 nm was also noted to have a high correlation with the experimental thermal response. This indicates that an impurity (possibly Fe^{3+}) absorbing at 255 nm is, or is linked with, the dominant cause of decreased thermal performance. When combined with other measurement techniques in this way, RTOA can be used to determine the extent to which a particular feature affects the overall material quality and thermal response.

RTOA is a simple and powerful technique that can be used to yield a fast and repeatable metric for the combined sum of material quality, with no reference materials. A single sample can either be compared to its ideal modeled behavior, or it can be ranked relatively within a set of samples. And while this demonstration was performed using doped materials, it is broadly applicable to many types of optical media, including undoped media, which are of use in high power optical systems. To the best of the authors' knowledge, no other technique exists which possesses RTOA's simplicity of experimental set up combined with its thermal modeling methodology. By using RTOA, the best optical materials can be quickly selected for processing, and ceramic fabrication methods can be easily refined in order to improve material quality.

Acknowledgments

The authors are pleased to acknowledge the support of the Trumpf USA, the Air Force Research Laboratory, the NDSEG Graduate Fellowship, the DEPS Graduate Fellowship, and the state of Florida.

#235182 - $15.00 USD Received 2 Mar 2015; revised 7 May 2015; accepted 8 May 2015; published 19 May 2015